Special Conference Edition November, 2017

http://dx.doi.org/10.4314/bajopas.v10i1.2S

Bayero Journal of Pure and Applied Sciences, 10(1):7 - 14
ISSN 2006 – 6996

GREEN SYNTHESIS OF ZINC NANOPARTICLES USING *Ipomoea asarifolia* LEAVES EXTRACT AND ITS ADSORPTION PROPERTIES FOR THE REMOVAL OF DYES

Ibrahim, M. B. and Abdullahi, S.H.
Department of Pure and Industrial Chemistry, Bayero University, P.M.B. 3011, Kano, Nigeria
mbibrahim.chm@buk.edu.ng:sagirwasai@gmail.com

ABSTRACT
In this paper, a green method is reported for the synthesis and characterization of zinc nanoparticles using Ipomoea asarifolia leaf extract as reducing and capping agent together with polyethylene glycol (PEG-10000) as stabilizing agent. The biosynthesized zinc nanoparticles were characterized by UV-Vis absorption spectroscopy, Fourier transform infrared spectroscopy (FT-IR), X-ray diffraction (XRD), and scanning electron microscopy (SEM); and were used as adsorbent for the removal of Bromophenol blue (BPB), and Eriochrome black T (EBT) dyes. Isotherms, kinetics and thermodynamics of the adsorption process were studied with the view to understand the adsorption mechanism. The adsorption isotherms were closely described by Freundlich isotherm model with correlation coefficient (R^2) of 0.99. The adsorption kinetics data were well fitted by the pseudo-second-order rate model with high regression coefficient (0.998). The intra particle diffusion of BPB anld EBT on ZnNPs represents the rate-limiting step. The adsorption capacity increases with the increase in temperature (from 298 to 318K) and thermodynamic calculations suggested that the adsorption of the dyes onto ZnNPs is an endothermic process with ΔH values of 10.78kJ/mol for BPB and 14.14 kJ/mol for EBT respectively.
Keywords: Adsorption, Bromophenol blue, Eriochrome black T, Ipomoea asarifolia, Zinc nanoparticles.

INTRODUCTION

Dyes are a major class of synthetic organic compounds released by many industries such as paper, plastic, leather, food, cosmetic, textile and pharmaceutical industries (Gundogdu *et al.,* 2009). The aromatic structures of these dyes make them highly resistant to light, biological activity, ozone and other degrading environmental conditions (Kaushik and Malik, 2009). Many techniques, such as adsorption, flocculation, electro-coagulation, UV-light degradation, and redox treatments, are being routinely used for abating dyes (Kumar *et al.,* 2011). Among these methods, adsorption is generally preferred for the removal of dye from aqueous solutions due to its high efficiency, easy handling, availability of different adsorbents and cost effectiveness. Various workers have exploited substances such as *Alibizia lebbeck* shell, water melon rind and neem tree leaves, activated carbon developed from fertilizer waste, bagasse fly ash, activated carbon fibers, wool carbonizing waste, clays, perlite, silica, wood meal, activated carbon developed from bamboo, alum sludge, and fly ash for this purpose (Ibrahim and Umar, 2016; Ibrahim and Sani, 2014; Balasubramani and Sivarajasekar, 2014). Adsorption based on application of various metallic and semi metallic nanoparticles are designed to clean up aqueous contaminated water in short time due to their unique properties in terms of high amount of surface atom, high mechanical stability, thermal strength, electrical conductivity, thermal conductivity, and high surface area (Wu *et al.,* 2004; Li *et al.,* 2013). The use of plant materials as eco friendly alternative for the synthesis of nanoparticles has proven advantageous, as it does not require high pressure, energy, and toxic chemicals (Philip *et al.,* 2011; Ahmad *et al.,* 2011). Few papers reported the biosynthesis of zinc oxide nanoparticles using plant extracts such as *Parthenium hysterophorus* (Rajiv *et al.,* 2013), *Poncirus trifoliate* plant dried fruits (Nagajyothi *et al.,* 2013), milky latex of *Calotropis procera* (Singh and Gopal, 2008), *Olea europea* (Awwad *et al.,* 2014), and *Aloe vera* extract (Sangeetha *et al.,* 2011). In this study, a novel green synthesis of zinc nanoparticles using *Ipomoea asarifolia* leaf extract as reducing and capping agent together with aqueous polyethylene glycol (PEG-10000) as stabilizing agent and its utilization as novel adsorbent for the removal of dyes is reported.

MATERIALS AND METHODS

***Ipomoea asarifolia* Leaves Sampling and Preparation of Extract**

The leaves of *Ipomoea asarifolia* plant (Fig 1) used in this study were collected behind Wasai Dam, Minjibir local area, Kano, Nigeria. The *Ipomoea asarifolia* collected were washed several times with distilled water to remove dust particles, and other impurities, dried under shade for 48 hours to remove residual moisture, and then ground into powder. 10.0g of the powdered leaves was placed in a 500cm^3 glass beaker containing 300cm^3 of distilled water. The mixture was boiled for 10 minutes at 90^{0}C. It was then cooled and centrifuged at 3500rpm in order to collect the pure leaves extract. The extract was stored in a cool dry place in an air tight container for further use.

Fig 1: Image of *Ipomoea asarifolia* leaves

Green Synthesis of Zinc Nanoparticles

Zinc nanoparticles were synthesized via a four step processes proposed by Caroling *et al.* (2015): The first step involve dissolving 3.22g of zinc sulphate pentahydrate (99.8%, Sigma Aldrich) in 1.0L of distilled water to prepare 0.02M $ZnSO_4$ solution. While the second is the addition of dissolved Polyethylene glycol (PEG) (Sigma Aldrich) to the aqueous solution of the zinc sulphate salt with vigorous stirring. In the third step, *Ipomoea asarifolia* leaves extract was added to the zinc sulphate solution containing PEG which serves as a capping agent and also prevents the nanoparticles formed from being oxidized to zinc oxide. In the last step 0.1M sodium hydroxide (99.8%, Sigma Aldrich) was added in drops to the solution under continuous rapid stirring, in order to adjust the pH. The instant colour change in the aqueous phase indicates that reduction has started to occur. Formation of zinc nanoparticles was shown by the formation of brown solution.

Characterization of Zinc Nanoparticles

UV-vis spectrum of the prepared nanoparticles was recorded, by taking 0.1 cm^3 of the sample and diluting it with 2cm^3 distilled water, using a Cary 50, version 3.0 spectrophotometer in the wave length region 300 to 800 nm operated at a resolution of 1 nm. Scanning electron microscopy (SEM) analysis of the synthesized nanoparticles was performed using, Leica Stereoscan-440, SEM machine. Powder X-ray diffraction was performed using a X-ray diffractometer, EMPYREAN- 2010, with CuKα radiation λ = 1.5405 Å over a wide range of Bragg angles ($4^o \leq 2\theta \leq 75^o$). Fourier transform infrared spectroscopic measurements were done using Cary 630 IR spectrophotometer from Agilent Technologies.

Batch Adsorption Studies

Batch adsorption experiment for the removal of Eriochrome Black T (EBT) and Bromophenol Blue (BPB) were carried out by agitating (0.1 to 0.8g) of the nanoparticles with 50cm^3 of the dyes in a 100cm^3 Erlenmeyer flask at constant temperature (298 to 318K) and at 250 rpm. The mixture was then centrifuged for 5 minutes at 3500 rpm and the supernatant was used for spectrophotometric analyses using UV-Visible spectrophotometer at the corresponding λ_{max} of each dye (591nm for BPB, and 514nm for EBT) respectively to determine the absorbance of the residual dye. The final concentration of the dyes after agitation was determined and the effects of agitation time (5 to 100 minutes), adsorbent dose (0.1 to 0.8g), initial dye loading concentration (10 to 50 ppm), pH (2 to 12) and temperature (298 to 318K)p on the adsorptive removal of the dyes were investigated.

The percentage of dye removal was calculated using equation (1), while equilibrium adsorption capacities from equation (2)

$$\%R = \frac{C_o - C_t}{C_o} \times 100 \quad \text{.....(1)}$$

$$q_e = \frac{(C_o - C_e)V}{W} \quad \text{.....(2)}$$

Where $C_0$and C_t and C_e are the initial and concentrations (mg/L) of the dyes initially, after time t and at equilibrium respectively. Vis the volume of the solution in L and W is the mass (g) of the nanoparticles (Ibrahim and Umar, 2016).

The experimental data were fitted to different models to evaluate and calculate the kinetics, thermodynamic, and isotherm parameters for the dye at desired pH. The solution pH was adjusted by the addition of dilute aqueous solutions of HCl and/or NaOH (0.1 M).

RESULTS AND DISCUSSION

UV-Vis spectra of zinc nanoparticles

The reduction of Zn^{2+} ions was monitored by UV-Vis spectrophotometer for the metal ion stability. The characterization of Zinc nanoparticles by UV-spectrophotometer was carried out in the range 300 to 800nm. The strong surface plasmon resonance (SPR) band positioned at 410 nm was observed for zinc nanoparticles (Fig 3). The position of SPR band in UV-vis spectra is sensitive to particle shape, size, its interaction with the medium, local refractive index and the extent of charge transfer between medium and the particles. The broad spectra indicate the presence of particles with a broad size distribution (Sosa *et al.*, 2003). Awwad *et al.* (2014) observed that the UV-vis absorption spectrum due to ZnO occurs nano-sheets at 374 nm in their effort to synthesize zinc oxide nanosheets using *Olea europea* leaf extract.

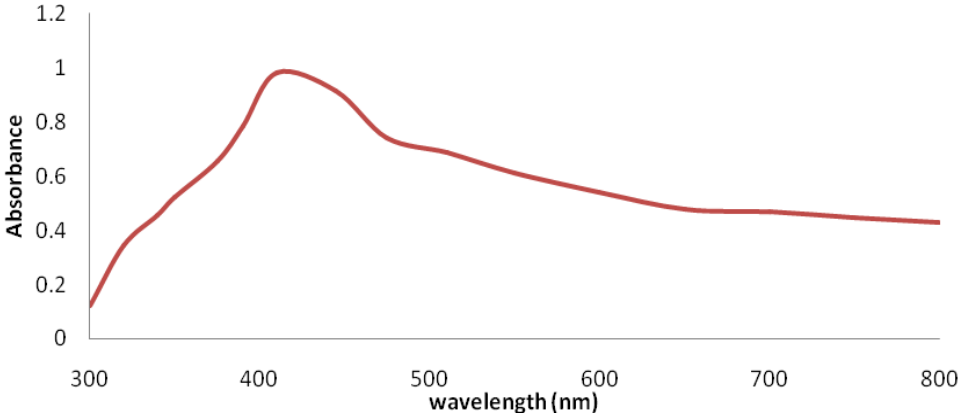

Fig 3: UV-vis spectra of zinc nanoparticles

FT-IR Spectra

FT-IR spectroscopy provides information on the surface functional groups of the ZnNPs and the local molecular environment of the capping agents on the nanoparticles. The FT-IR spectrum of *Ipomoea asarifolia* mediated ZnNPs is as shown in Fig 4. Absorption bands at 2853 cm^{-1} corresponds to C-H saturated stretching vibration, peaks at 1609cm^{-1}, 1500cm^{-1} and 1417cm^{-1} for aromatic stretching frequencies and peak at 3172cm^{-1} corresponds to SP^2 C-H stretching. All these bands clearly confirm the presence of polyphenols, proteins, tannins and flavonoids in *Ipomoea asarifolia* which act as reducing agents for the synthesis of zinc nanoparticles. Thus, the IR spectroscopic study confirmed that the *Ipomoea asarifolia* has the ability to perform dual functions of reduction and stabilization of ZnNPs.

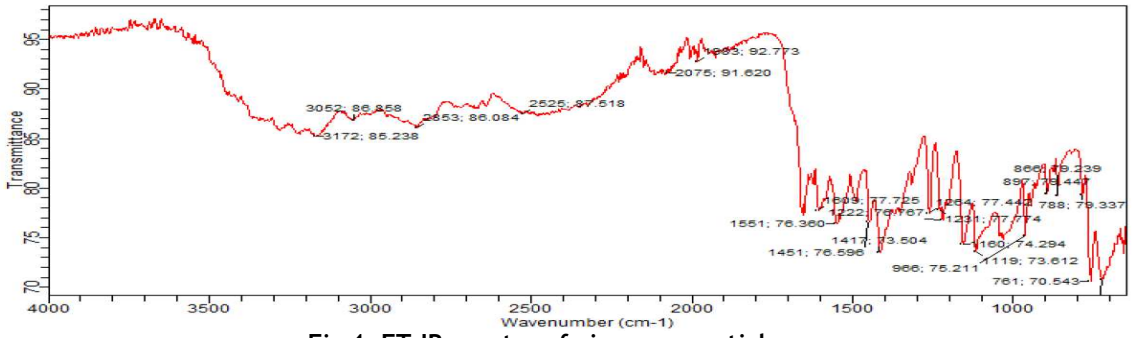

Fig 4: FT-IR spectra of zinc nanoparticles

Scanning Electron Microscopy (SEM)

The synthesized nanoparticles morphology was characterized by scanning electron microscope (SEM) using Stereoscan 440 SEM machine. After the completion of reaction, the nanoparticles placed on carbon coated copper grid exhibited different geometries (Fig 5).

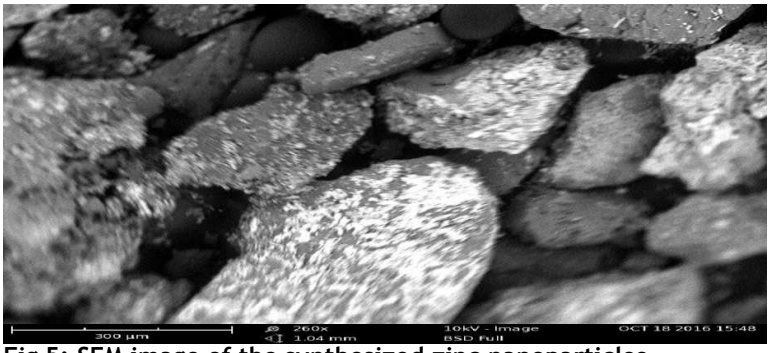

Fig 5: SEM image of the synthesized zinc nanoparticles

X-ray Diffraction Studies (XRD)

X-ray diffraction (XRD) pattern of zinc nanoparticles powder (Fig 6) exhibits peaks at 2θ angles of 30.0241°, 35.6626°, 37.8010° and 44.0259° that correspond to the lattice plane {100}, {002}, {101} and {102}. From the full-width at half maximum of diffraction peaks, the average size of the nanoparticles based on Debye-Scherrer equation (Gurusamy and Cellapandian, 2013) was around 39.15 nm.

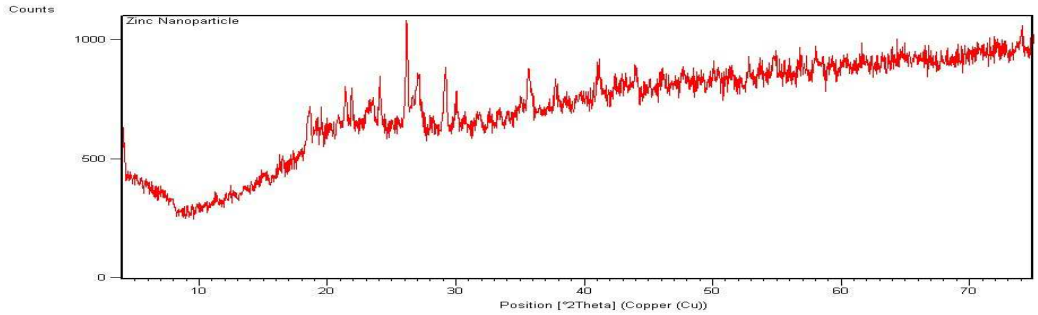

Fig 6: XRD spectra of the synthesized zinc nanoparticles

Effect of Contact Time

The contact time's needs for EBT and BPB solutions to reach equilibrium were 40 and 60 minutes with percentage dye removal of 71.05% and 61.75% respectively. The studies involving different contact times help in determining the uptake capacities of the dye at varying time intervals keeping the amount of the adsorbents fixed at room temperature (Karimi *et al.*, 2012).

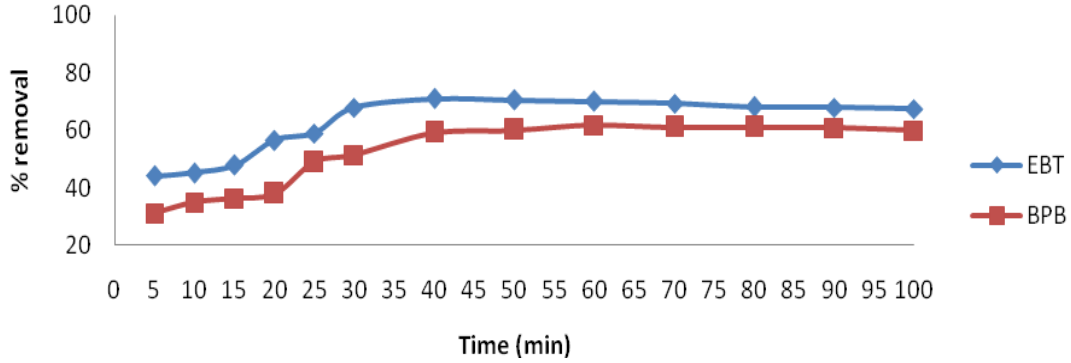

Fig 7: Effect of contact time on the adsorption of EBT and BPB on to the Zn nanoparticles

Effect of adsorbent dosage

The effect of Zn-NPs dosage on the removal of BPB and EBT are shown in Fig 8. The initial removal percentage for the removal of BPB increases rapidly with the increase in the amount of zinc nanoparticles and after 0.4g the removal percentage slightly decline. The BPB removal percentage increased from 60.75% to 79.31% with the increase in the amount of adsorbent from 0.1 to 0.4g. Similarly, for EBT there is significant increase in adsorption (from 69.9% to 84.52%) with increasing mass of the adsorbent from 0.1 to 0.5g, the adsorption process was then decreased with further increase in the adsorbent dose to 0.7g from where the adsorption process slightly rises further till 0.8g with percentage removal about 83.4%. Therefore 0.4 and 0.5g was chosen for the adsorption of BPB and EBT respectively.

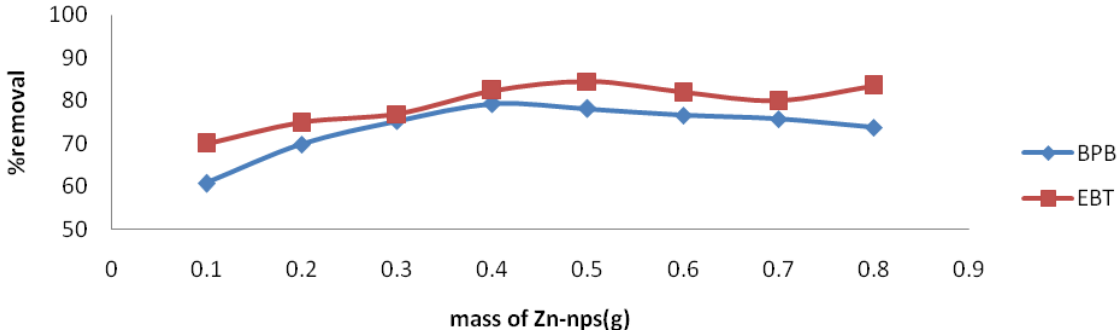

Fig 8: Effect of adsorbent dosage on the adsorption of BPB and EBT onto Zn nanoparticles

Effect of Initial Dye Loading Concentration

Effect of BPB and EBT initial concentrations on the efficiency of its adsorption was investigated in the range of 10 to 50 mg L^{-1} and the results are as shown in Fig 9. Although, by increasing the initial dye concentration the percentage of dye removal decreased, the actual amount of dye adsorbed per unit mass of Zn-NPs was found to increase.

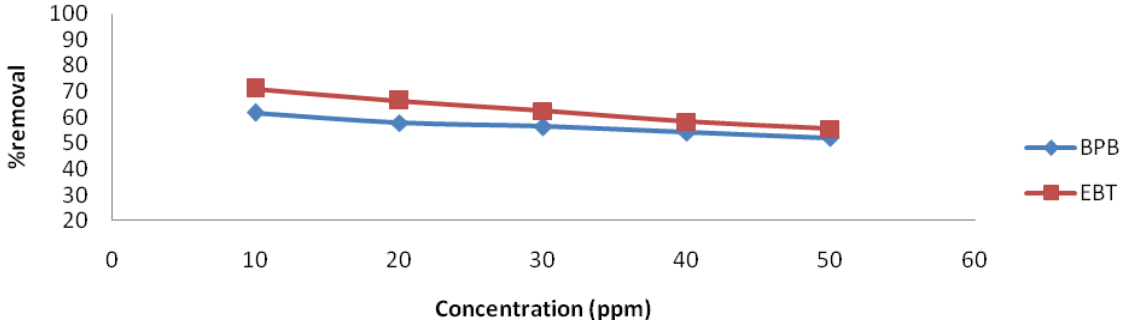

Fig 9: Effect of initial dye concentration on the adsorption of BPB and EBT onto Zn nanoparticles

Effect of pH

In this research the pH of the dyes was varied from 2 to 12 while other parameters such as time, adsorbent dose, temperature, were kept constant. Effect of pH on the removal of BPB and EBT is as shown in Fig 10. Increase in the pH (from 2 to 12) causes a significant decrease in the percentage removal of BPB and EBT (from 90.31% to 71.08% for EBT and from 89.56% to 70.02% for BPB). This may be attributed to the fact that at low pH values functional groups on the biosynthesized zinc nanoparticles are protonated and consequently becomes positively charged which can interact with the negatively charged BPB and EBT dyes, due to electrostatic attractions adsorption process is favoured which lead to high percentage removal. At higher pH, the acidic group of dye molecule becomes negatively charged. The electrostatic repulsion between the negatively charged dye and negative charges present on the nanoparticles is made higher; this may result in a decrease in the degree of adsorption of dye molecules.

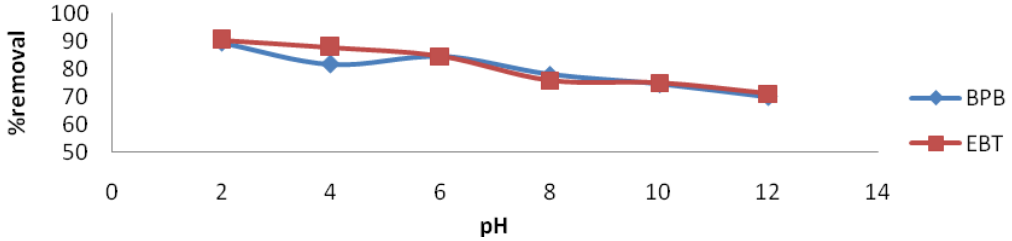

Fig 10: Effect of pH variation on the adsorption of BPB and EBT onto Zn nanoparticles

Effect of Temperature

In this research the effect of temperature was studied by varying the temperature from 298K, 308K and 318K. The results of effects of temperature on the adsorption of BPB and EBT are as shown in figure 11. The result shows that adsorption process increases with increase in temperature and reached a maximum value at 318K. This may be explained on the basis that elevating the temperature leads to the dislodging of the solvent molecule (water) from interfacial region thereby providing and exposing more number of adsorption sites.

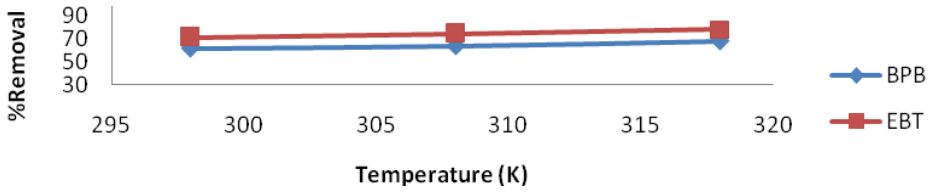

Fig 12: Effect of temperature on the adsorption of BPB and EBT onto Zn nanoparticles

Kinetics and Adsorption Isotherms of BPB and EBT onto Zn nanoparticles

Conventional kinetic models including pseudo-first-order, second-order kinetic models, intraparticle diffusion model and Elovich equation were applied in this research for testing the experimental data. The results were as contained in Table 1. Three isotherm models were tested and the isotherm parameters were as contained in Table 2. Based on the information from the Table, R^2 value of the Freundlich isotherm model was higher than the other models, this show that the experimental equilibrium data was better explained by the Freundlich equation.

Table 1: Adsorption kinetics parameters of BPB and EBT on zinc nanoparticles

Model	Parameter	Value	
		BPB	EBT
Pseudo First order: $\log (q_e - q_t) = \log q_e - \left(\frac{K1}{2.303}\right) t$	K_1	0.040	0.035
	$q_{e\ (calc)}$	1.780	1.590
	R^2	0.680	0.390
Pseudo Second order: $\frac{t}{q_t} = \frac{1}{K_2 q_e^2} + \frac{1}{q_e} t$	K_2	0.032	0.069
	$q_{e\ (calc)}$	3.390	3.600
	R^2	0.990	0.990
Elovich equation: $q_t = \frac{1}{\beta} \ln (\alpha \beta) + \frac{1}{\beta} \ln (t)$	α	1.190	7.130
	B	1.630	1.990
	R^2	0.890	0.810
Intraparticle diffusion: $q_t = k_{diff} t^{1/2} + C$	k_{diff}	0.220	0.170
	C	1.190	2.020
	R^2	0.840	0.690

Key: k_1 : Pseudo first order rate constant
q_e: Equilibrium adsorption capacity
q_t: Adsorption capacity at time t
t: Adsorption time
α and ß: Elovich constants
k_{diff}: Intraparticle diffusion rate constant
C: Intercept which is related to the thickness of the boundary layer

Table 2: Various isotherm models and their calculated parameters

Isotherm Equation	Parameters	BPB	EBT
Langmuir: $\frac{C_e}{q_e} = \frac{1}{K_L Q_m} + \frac{C_e}{Q_m}$	Q_m (mgg^{-1})	34.60	24.69
	K_L (Lmg^{-1})	0.024	0.056
	R_L	0.450	0.260
	R^2	0.980	0.990
Freundlich: $\log q_e = \log K_f + \frac{1}{nf} \log C_e$	$1/n_f$	0.790	0.669
	K_f ($(mgg^{-1})/(mgl^{-1})^{1/n}$)	1.077	1.796
	R^2	0.990	0.990
Temkin: $q_e = B_T \ln K_T + B_T \ln C_e$	B_T($Jmol^{-1}$)	5.360	5.020
	K_T (Lg^{-1})	0.409	0.630
	R^2	0.970	0.980

Key: K_L: Langmuir constant
Q_m: Maximum adsorption capacity
K_f: Freundlich constant
$1/ n_f$: Adsorption intensity
B_T: Temkin constant related to heat of adsorption
K_T: Equilibrium binding constant

An ideal adsorbent for the treatment of wastewater must not only have a large adsorption capacity but it has to have fast adsorption rate as well. It can be observed that the adsorption process follows Pseudo second order kinetics since it has higher linear regression coefficient value (0.990) for all the studied dyes.

Adsorption Thermodynamics of BPB and EBT onto Zn nanoparticles

Thermodynamic studies were performed to find out the nature of adsorption process. Thermodynamic parameters such as standard free energy change (ΔG^o), enthalpy change (ΔH^o) and entropy change (ΔS^o) were calculated and tabulated in Table 3. Negative ΔG^o values suggested that the adsorption of all the dyes from aqueous solution onto the Zn-NPs was spontaneous in nature. Positive ΔH^0 values confirm that the adsorption process is endothermic in nature; also lower values of ΔH^0 suggest that the adsorption process is physical. Moreover, positive values of ΔS^0 values showed the increase in the affinity of the dyes onto Zn-NPs.

Table 3: Adsorption thermodynamics parameters

Dyes	ΔH^0 (kJ/mol)	ΔS^0 ($Jmol^{-1}K^{-1}$)	ΔG^0(kJ/mol)		
			298K	308K	318K
BPB	10.78	39.97	-1.131	-1.531	-1.930
EBT	14.14	54.86	-2.208	-2.757	-3.305

CONCLUSION

The nanoparticles were found to be effective in removal of the dyes (BPB and EBT) from aqueous solution following pseudo-second-order kinetic model; thus it is recommended to be used for the removal of dyes from aqueous solutions.

REFERENCES

Ahmad, N, S. Sharma, V. N. Singh, S. F. Shamsi, A. Fatma and B. R. Mehta (2011). Room temperature biosynthesis of silver nanoparticles using *Desmodium trifolium* extract *Biotechnol. Res. Int.* 454090

Awwad, M., Borhan, A., Ahmad, L., (2014): Green synthesis, characterization and optical properties of zinc oxide nanosheets using *Oleaeuropea* leaf extract. *Adv. Mat. Lett*.5(9), 520-524.

Balasubramani, K., and Sivarajasekar, N. (2014).Adsorption Studies of Organic Pollutants onto activated Carbon. *International Journal of Innovative Research in Science, Engineering and Technology*. 3:10575- 10581

Caroling, G., E. Vinodhini, A. Mercy, R., and Shanthi, P. (2015). Biosynthesis of Copper Nanoparticles Using Aqueous Phyllanthus Embilica (Gooseberry) Extract- Characterisation and Study of Antimicrobial Effects. *Int. J. Nano. Chem.***1**, (2):53-63.

Gundogdu, A., Ozdes, D.; C. Du ran, VN.;Bulut, M. and Soylak, H. B. (2009). Biosorption of Pb(II) ions from aqueous solution by pine bark (Pinusbrutia Ten.)" *Chemical Engineering Journal* 153:62-69.

Gurusamy, A., and Cellapandian, K (2013). "Green Synthesis of Silver Nanoparticles using Millingtonia hortensis and Evaluation of their Antimicrobial Efficacy", *Inter.j.nanomater.bios*, 3 (1):21-25.

Ibrahim, M. B., and Umar, A. (2016). Adsorption thermodynamics of some basic dyes uptake from aqueous solution using Alibizia lebbeck shells. *Chemsearch Journal* 7(1):43-51.

Ibrahim, M. B., Sani, S. (2014). Comparative Isotherms Studies on Adsorptive Removal Of Congo Red From Wastewater By Watermelon Rinds And Neem-Tree Leave. *Open Journal Of Physical Chemistry,* 139-146.

Karimi, H., Mousavi, S., and Sadeghian, B. (2012). Silver nanoparticles loaded on activated carbon as efficient adsorbent for removal of methyl orange. *Indian Journal of Science and Technology,* 5(3): 2346-2353.

Kaushik, P. and Malik, A. (2009). Fungal dye decolourization: Recent advances and future potential. *Environmental International,* 35:127-214.

Kumar, A., Choudhary, P., and Verma, P. A. (2011). A comparative study on the treatment methods of textile dye effluents. *Global Journal of Environmental Research* 5:46-50-52.

Li, X., L. Zheng, L. Huang, O. Zheng, Z. Lin, L. Guo, B. Qiu, G. Chen, (2013). Adsorption removal of crystal violet from aqueous solution using a metal-organic frameworks material, copper coordination polymer with dithiooxamide, *J. Appl. Polym. Sci.* 129(5):2857–2864.

Nagajyothi, P. C.; An, T. N. M.; Sreekanth, T. V. M.; Lee, D. J.; Lee, K. D. (2013). Green route biosynthesis: characterization and catalytic activity of ZnO nanoparticles. *Mater. Lett.*108:160-163

Philip, D., Unni, C., Aromal, S. A., and Vidhu, V. K. (2011). Murraya Koenigii leaf assisted green synthesis of silver and gold nanoparticles. *Spectrochim. Acta, Part A*. 78:899–904.

Rajiv, P.; Rajeshwari, S.; Venckatesh, R (2013). Bio-fabrication of zinc oxide nanoparticles using leaf extract of Parthenium hysterophorus L. and its size-dependent antifungal activity against plant pathogens. *Spectrochimica Acta Part A: Molecular and Biomolecular Spectroscopy*. 112: 384-387.

Sangeetha, G.; Rajeshwari, S. and Venckatesh, R. (2011). Green synthesis of zinc oxide nanoparticles by aloe barbadensis miller leaf extract: Structure and optical properties. *Mater. Res. Bull.* 46:2560–2566.

Singh, S. C.; Gopal, R. (2008). Synthesis of colloidal zincoxide nanoparticles by pulsed laser ablation in aqueos media. *Physica E*: Low-dimensional Systems and Nanostructures., 40: 724-730.

Sosa, I. O., Noguez, C., and Barrera, R. G., (2003). "Optical properties of metal nanoparticles with arbitrary shapes", *J. Phys. Chem,* 107: 6269– 6275.

Walker, G. M., Hansen, L., Hanna, J. A., Allen, S. J., (2003). Analysis of the sorption efficiency of acid, basic, and direct dyes using Chitosan, fly ashes immobilized onto chitosan and modified saw dust immobilized onto chitosan as sorbents. *Journal of Water Resources.*37 :2081-2089.

Wu, Z., H. Joo, I.-S. Ahn, S. Haam, J.-H. Kim, K. Lee, (2004). Organic dye adsorption on mesoporous hybrid gels, *Chem. Eng. J.* 102: 277–282.